

1 **Astrocytes modulate thalamic sensory processing via mGlu2**
2 **receptor activation**
3
4

5 To appear in: *Neuropharmacology*

6 Received Date: 4 August 2016

7 Revised Date: 27 March 2017

8 Accepted Date: 13 April 2017

9

10 **C.S. COPELAND^{1,2}, T.M. WALL³, R.E. SIMS⁴, S.A. NEALE⁵, E. NISENBAUM³, H.R. PARRI⁴,**
11 **T.E. SALT¹**

12 ¹ INSTITUTE OF OPHTHALMOLOGY, UNIVERSITY COLLEGE LONDON, 11-43 BATH STREET, LONDON, EC1V 9EL, UK

13 ² ST GEORGE'S, UNIVERSITY OF LONDON, CRANMER TERRACE, LONDON, SW17 0RE, UK,

14 ³ ELI LILLY AND COMPANY, 893 S DELAWARE STREET, INDIANAPOLIS, IN 46285, USA

15 ⁴ SCHOOL OF LIFE AND HEALTH SCIENCES, ASTON UNIVERSITY, BIRMINGHAM, B4 7ET, UK

16 ⁵ NEUREXPRT LIMITED, KEMP HOUSE, 152-160 CITY ROAD, LONDON, EC1V 2NX, UK

17

18 **ABSTRACT**

19 Astrocytes possess many of the same signalling molecules as neurons. However, the role of
 20 astrocytes in information processing, if any, is unknown. Using electrophysiological and imaging
 21 methods, we report the first evidence that astrocytes modulate neuronal sensory inhibition in the
 22 rodent thalamus.

23

24 We found that mGlu2 receptor activity reduces inhibitory transmission from the thalamic reticular
 25 nucleus to the somatosensory ventrobasal thalamus (VB): mIPSC frequencies in VB slices were
 26 reduced by the Group II mGlu receptor agonist LY354740, an effect potentiated by mGlu2 positive
 27 allosteric modulator (PAM) LY487379 co-application (30nM LY354740: 10.0±1.6% reduction; 30nM
 28 LY354740 & 30µM LY487379: 34.6±5.2% reduction).

29

30 We then showed activation of mGlu2 receptors on astrocytes: astrocytic intracellular calcium levels
 31 were elevated by the Group II agonist, which were further potentiated upon mGlu2 PAM
 32 coapplication (300nM LY354740: ratio amplitude 0.016±0.002; 300nM LY354740 & 30µM LY487379:
 33 ratio amplitude 0.035±0.003).

34

35 We then demonstrated mGlu2-dependent astrocytic disinhibition of VB neurons *in vivo*: VB neuronal
 36 responses to vibrissae stimulation trains were disinhibited by the Group II agonist and the mGlu2
 37 PAM (LY354740: 156±12% of control; LY487379: 144±10% of control). Presence of the glial inhibitor
 38 fluorocitrate abolished the mGlu2 PAM effect (91±5% of control), suggesting the mGlu2 component
 39 to the Group II effect can be attributed to activation of mGlu2 receptors localised on astrocytic
 40 processes within the VB.

41

42 Gating of thalamocortical function via astrocyte activation represents a novel sensory processing
 43 mechanism. As this thalamocortical circuitry is important in discriminative processes, this
 44 demonstrates the importance of astrocytes in synaptic processes underlying attention and cognition.

45 **KEY WORDS:** astrocyte; metabotropic glutamate receptor subtype 2; synaptic inhibition; thalamus;
 46 thalamic reticular nucleus

47

48 **ABBREVIATIONS**

49 AMPA, α -Amino-3-hydroxy-5-methyl-4-isoxazolepropionic acid; CNQX, 6-cyano-7-nitroquinoxaline-2,3-dione; DL-APV, DL-2-Amino-5-
 50 phosphonopentanoic acid; DMSO, dimethyl sulfoxide; GABA, gamma amino butyric acid; i.p., intraperitoneal; LY341495, (2S)-2-Amino-2-
 51 [(1S,2S)-2-carboxycycloprop-1-yl]-3-(xanth-9-yl)propanoic acid; LY354740, (1S,2S,5R,6S)-2-Aminobicyclo[3.1.0]hexane-2,6-dicarboxylic acid;
 52 LY487379, 2,2,2-Trifluoro-N-[4-(2-methoxyphenoxy)phenyl]-N-(3-pyridinylmethyl)ethanesulfonamide hydrochloride; mGlu, metabotropic
 53 glutamate; mGlu2, metabotropic glutamate receptor subtype 2; mGlu3, metabotropic glutamate receptor subtype 3; mIPSC, miniature
 54 inhibitory post-synaptic current; NaCl, sodium chloride, NIH, National Institutes of Health; NMDA, N-methyl-D-aspartate; PAM, positive
 55 allosteric modulator; PSTH, post-stimulus time histogram; ROI, region of interest; SEM, standard error of the mean; SR101, Sulforhodamine
 56 101; TRN, thalamic reticular nucleus; TTX, tetrodotoxin; VB, ventrobasal thalamus.

57

58 1.0 INTRODUCTION

59 The thalamic reticular nucleus (TRN) is responsible for ensuring synchronous activity across specific
60 thalamo-cortical circuits required for sensory perception or the preparation and execution of distinct
61 motor and/or cognitive tasks. It is therefore imperative to ascertain how inhibition from the TRN to
62 thalamic nuclei is controlled to understand how neurophysiological disease states associated with TRN
63 malfunction precipitate (Huguenard, 1999; Rub *et al.*, 2003; Barbas & Zikopoulos, 2007; Pinault, 2011).

64

65 The TRN surrounds the entire anteroposterior extent of the dorsal thalamus, meaning all thalamo-
66 cortical and cortico-thalamic projections must pass through and make connections with its mesh of
67 inhibitory interneurons (Houser *et al.*, 1980; Jones, 1985) (**FIG. 1**). This strategic localisation between
68 thalamus and cortex enables the TRN to mediate coherent activity patterns within the thalamo-
69 cortico-thalamic excitatory loop by providing both feedback and feedforward inhibition to thalamic
70 nuclei upon thalamo-cortical and cortico-thalamic input, respectively (Shosaku *et al.*, 1989) (**FIG. 1**).

71 The Group II metabotropic glutamate (mGlu) receptors (mGlu2/3) modulate physiologically-evoked
72 responses in the somatosensory ventrobasal thalamic nucleus (VB) by reducing inhibition from the
73 TRN (Salt & Turner, 1998; Copeland *et al.*, 2012), with the mGlu2 component to this Group II effect
74 likely activated by glutamate spillover upon physiological sensory stimulation (Copeland *et al.*, 2012).

75

76 VB astrocytes *in vitro* can respond to sensory afferent stimulation with an elevation in intracellular
77 calcium (Parri *et al.*, 2010), in accordance with astrocytic activation in other brain regions (Porter &
78 McCarthy, 1996; Grosche *et al.*, 1999; D'Ascenzo *et al.*, 2007). These elevations can initiate release of
79 gliotransmitters including glutamate (Fellin *et al.*, 2004), D-serine (Panatier *et al.*, 2006), adenosine
80 triphosphate (Guthrie *et al.*, 1999) and adenosine (Winder *et al.*, 1996), with subsequent modulation
81 of neuronal excitability and synaptic transmission (Fellin *et al.*, 2004; Serrano *et al.*, 2006). Astrocytic
82 processes co-localise with sensory and TRN afferent terminals around the soma and proximal
83 dendrites of VB neurons (Ralston, 1983; Ohara & Lieberman, 1993); thus, it is important to understand

84 how astrocytes are activated as concomitant gliotransmission may represent a significant mechanism
85 in the regulation of thalamo-cortical network function via modulation of the TRN-VB synapse.

86

87 Here, by firstly using *in vitro* electrophysiology we confirmed the presence of an mGlu2 component to
88 the overall Group II mGlu receptor effect on inhibitory synaptic transmission from the TRN to the VB,
89 as previously indicated *in vivo* (Copeland *et al*, 2012). By then using *in vitro* calcium imaging, which
90 enabled the identification of the cellular foundation supporting this mechanism, the mGlu2
91 component was identified as astrocyte-dependent: mGlu2 receptor activation elicited elevations in
92 astrocytic (but **not** neuronal) intracellular calcium - a novel mechanism of astrocyte activation. Finally,
93 we identified VB neurons responsive to trains of single vibrissa stimuli *in vivo* and applied selective
94 compounds locally. We delineate that the mGlu2 receptor astrocyte-dependent mechanism
95 contributes to the modulation of sensory transmission in a physiological context. Together, the data
96 indicate that the mGlu2 component to the Group II mGlu receptor effect is purely astrocyte-
97 dependent, making astrocytes an integral signalling intermediary in sensory processing.

98 **2.0 MATERIAL AND METHODS**

99 **2.1 ETHICAL APPROVAL**

100 All experimental conditions and procedures were either in accordance with the National Institutes of
101 Health (NIH) regulations of animal care covered in the Principles of Laboratory Animal Care, NIH
102 publication 85-23, revised 1985, and were approved by the Eli Lilly and Company Institutional Animal
103 Care and Use Committee, or were approved by the Home Office (UK) and were in accordance with the
104 UK Animals (Scientific Procedures) Act 1986 and associated guidelines.

105

106 **2.2 *IN VITRO* ELECTROPHYSIOLOGY**

107

108 **2.21 ANIMALS**

109 Male Sprague-Dawley rats (12–18 days old; Harlan, Indianapolis, USA, n=10) were deeply
110 anaesthetised with 4.0% isoflurane and decapitated into a container of crushed ice.

111

112 **2.22 SLICE PREPARATION AND MAINTAINING SOLUTIONS**

113 The brain was quickly removed and placed in an oxygenated, ice cold beaker of slicing solution which
114 contained (in mM): 110 NaCl; 10 MgCl₂; 2 KCl; 26 NaHCO₃; 1.25 NaH₂PO₄; 0.5 CaCl₂; 10 HEPES and 15
115 glucose (pH adjusted to 7.45 with NaOH, osmolarity was 308 to 312 mOsm). After cooling in slicing
116 solution for 2 to 3 minutes, the whole brain was blocked (portions of anterior and posterior tissue
117 removed) using a razor blade and then glued to the microslicer (DTK Zero 1, DSK) tray using
118 cyanoacrylate. The tray containing the blocked and mounted brain was filled with oxygenated, ice cold
119 slicing solution and serial, coronal sections were cut at a thickness of 300µm. Slices were then placed
120 in a larger recovery chamber containing oxygenated slicing solution at room temperature (18 to 20°C).

121 The recovery chamber was in a large water bath, which was initially at room temperature. After a 10
122 minute period, 500 μ L of 0.5M CaCl₂ solution was slowly added to the recovery chamber (500ml
123 volume) to increase the calcium concentration to 1mM. The water bath was then turned on and the
124 temperature was monitored inside the recovery chamber. The recovery chamber temperature was
125 allowed to reach 33 to 34°C for a period of approximately 30 minutes, after which the water bath was
126 turned off and the recovery chamber was allowed to slowly return to room temperature (18 to 20°C).
127 Slices were used for recording after at least 1 hour of recovery time.

128

129 2.23 RECORDING CONDITIONS

130 Slices were placed in a superfusion chamber mounted on a Nikon Eclipse FN-1 microscope. Neurons
131 within the VB area of the thalamus were visualized using IR/DIC water immersion optics. The recording
132 solution was composed of (in mM): 115 NaCl; 1.5 MgCl₂; 5 KCl; 26 NaHCO₃; 1.25 NaH₂PO₄; 10 HEPES;
133 2 CaCl₂ and 15 glucose at pH 7.45, oxygenated with carbogen gas (95%O₂/5%CO₂) and osmolarity of
134 300 to 305 mOsm. The brain slice in the chamber was continually superfused at a rate of 3mL/min
135 with oxygenated recording solution (18 to 20°C). Compound containing solutions were applied to the
136 slice via whole chamber superfusion. Glass recording electrodes were filled with (in mM): 140 CsCl; 1
137 MgCl₂; 10 HEPES; 3 NaATP; 0.3 NaGTP; 1 Cs-EGTA at pH 7.2 and osmolarity adjusted to 294 to 300
138 mOsm and had a resistance of 2 – 4M Ω .

139

140 2.24 EXPERIMENTAL PROTOCOL

141 Visualized neurons were patch clamped in whole cell configuration (Multiclamp 700B, MDS) and
142 access resistance (Ra) was evaluated in voltage clamp mode. A gapfree protocol (Clampex V10, MDS)
143 with a holding potential of -70mV was used to record miniature synaptic events until the access
144 resistance and holding current were stable in recording solution only. The slice was then superfused
145 with recording solution containing 10 μ M 6-cyano-7-nitroquinoxaline-2,3-dione (CNQX; Tocris), 50 μ M
146 DL-2-Amino-5-phosphonopentanoic acid (DL-APV; Tocris) and 0.5 μ M tetrodotoxin (TTX; Abcam) to

147 block the AMPA- and NMDA- evoked miniature and large amplitude events due to direct action
148 potential firing of inhibitory neurons, respectively, leaving only the GABA mediated miniature synaptic
149 events (confirmed in preliminary experiments by complete blockade of remaining synaptic events with
150 10 μ M bicuculline). LY354740, LY341495 and LY487379 (all made in-house) stocks were made in 100%
151 DMSO at 1000X the desired working concentration. Compounds were diluted into the recording
152 solution containing CNQX, APV and TTX immediately before application to the brain slice. All solutions
153 applied to the brain slices contained 0.1% to 0.2% DMSO. DMSO content was matched between
154 solutions for each experimental protocol. Compound treatment periods were from 10 to 12 minutes
155 in duration.

156

157 2.25 DATA COLLECTION AND STATISTICAL ANALYSIS

158 The frequency of the GABAergic miniature synaptic events was determined during the final 5 minutes
159 of each treatment period (baseline, 30nM LY354740, 100nM LY354740, 100nM LY354740 + 100nM
160 LY341495, 30nM LY354740 + 30 μ M LY487379, and 30 μ M LY487379) using the MiniAnalysis program
161 (V6.0.4, Synaptosoft). Inter-event intervals were calculated and plotted as cumulative fraction
162 histograms for each treatment group. The Kolmogorov-Smirnov test was performed on the inter-event
163 interval cumulative fractions to determine statistical significance of compound effects on spontaneous
164 GABAergic synaptic event activity.

165

166 2.3 INTRACELLULAR CALCIUM IMAGING

167

168 2.31 ANIMALS

169 Male juvenile Wistar rats and mice (10–16 days old; n=5; bred in house) were killed by halothane
170 overdose followed by cervical dislocation. IP3 R2 Knockout Mice (Ju Chen, UCSD) were bred from
171 founder mice kindly obtained from A. Araque, Instituto Cajal, Madrid. Mice were bred on a C57Bl6

172 background. WT^s (-/-) were bred from Heterozygous (+/-) bred pairs. Genotyping was conducted by
173 Transnetyx (Cordova, TN, USA).

174

175 2.32 SLICE PREPARATION AND MAINTAINING SOLUTIONS

176 Slices were prepared as described previously (Parri & Crunelli, 2001). Briefly, following removal from
177 the skull, the brain was glued with cyanoacrylate adhesive to a metal block and submerged in the bath
178 of Microm MV (Zeiss, Welwyn Garden City, UK) tissue slicer. The bathing solution was of the following
179 composition (in mM): NaCl 120, NaHCO₃ 16, KCl 1, KH₂PO₄ 1.25, MgSO₄ 5, CaCl₂ 1, glucose 10, and was
180 maintained at 5°C. Thalamic slices (350µm) were cut in the horizontal plane, and then stored in a 95%
181 O₂/5% CO₂ bubbled solution of identical composition at room temperature.

182

183 Following a 1h recovery period, experiments were performed in a solution of the following
184 composition (in mM): NaCl 120, NaHCO₃ 16 or 25, KCl 2, KH₂PO₄ 1.25, MgSO₄ 1, CaCl₂ 2, glucose 10, at
185 room temperature (20–24°C), unless otherwise stated. TTX (0.5µM) was included in the perfusate to
186 block sodium currents in VB neurons (Parri and Crunelli, 1998). Compounds LY354740, LY487379 and
187 MPEP were obtained from Tocris (Bristol, UK), Suramin from Sigma-Aldrich.

188

189 2.33 FLUORESCENCE IMAGING

190 Slices were loaded with either Fura-2 or Fluo4-AM (Invitrogen) dye (5µM with 0.01% pluronic acid)
191 after a post-cutting recovery period of 1 hour. Fluo4 was routinely used in experiments to monitor
192 Group II mGlu receptor activation, Fura-2 was used in dose response determination experiments
193 where comparison of repetitive drug applications in the same astrocytes was required. Astrocytes and
194 neurons were distinguishable by their morphological profiles: VB neurons have large somas (18µm
195 diameter), with 3-4 dendrites; astrocytes have much smaller somas (~8µm) with nebulous processes
196 (Parri *et al.*, 2001). Slices were also loaded with 1µM Sulforhodamine 101 (SR101), according to

197 published *in vitro* methods (Kafitz *et al.*, 2008) for verification of astrocyte identity. The recording
198 chamber and manipulators were mounted on a motorized moveable bridge (Luigs and Neumann) and
199 fluorescence dyes were excited using an Optoscan monochromator system, fitted to a Nikon FN1
200 upright microscope; filter cubes for selective Fura-2, Fluo4 and SR101 imaging were obtained from
201 Chroma. Images of slice areas of 444 μ m x 341 μ m were routinely acquired every 5s with a x20 objective
202 lens (NA=0.8) using an ORCA ER CCD camera (Hamamatsu) and analysed using Simple PCI software
203 (Hamamatsu). Fluorescence values over time for specific regions of interest (ROIs) were exported and
204 analysed using Sigmaplot (Systat). The number of events during a recording was determined by
205 identifying events where amplitude exceeded 2 standard deviations of baseline variations. For
206 determination of amplitude changes, the absolute ratio or ΔF increases in the different conditions in
207 the same cells were directly compared, so providing an internal control.

208

209 2.34 STATISTICAL ANALYSIS

210 All quantitative data are expressed in the text as mean (\pm SEM). Statistical tests included Student's t-
211 test and the Kolmogorov–Smirnov test for cumulative population distributions, as indicated.

212

213 **2.4 *IN VIVO* SINGLE NEURON RECORDING AND IONTOPHORESIS**

214

215 2.41 ANIMALS

216 All experiments were conducted using adult male Wistar rats (340-540g, n=18). Animals (Harlan, UK)
217 were housed on a 12h light/dark cycle with food and water *ad libitum*.

218

219 2.42 SURGERY

220 Animals were anaesthetised with urethane (1.2g/kg intraperitoneal [i.p.] injection) and were
221 prepared for recording as previously described (Salt, 1987, 1989). Throughout the experiments,
222 electroencephalogram and electrocardiogram were monitored. Additional urethane anaesthetic was
223 administered i.p. as required, and the experiment was terminated with an overdose of the same
224 anaesthetic.

225

226 2.43 RECORDING AND IONTOPHORESIS

227 Seven-barrel recording and iontophoretic glass pipettes were advanced into the VB. Extracellular
228 recordings were made from single VB neurons responsive to somatosensory input through the central
229 barrel (filled with 4M sodium chloride [NaCl]). Iontophoretic drug applications were performed using
230 the outer barrels (Salt, 1987, 1989). On each occasion, one of the outer barrels was filled with 1M NaCl
231 for current balancing. The remaining outer barrels each contained one of the following substances: N-
232 methyl-D-aspartate (NMDA; 50mM, pH8.0 in 150mM NaCl), (1S,2S,5R,6S)-2-
233 Aminobicyclo[3.1.0]hexane-2,6-dicarboxylic acid (LY354740; 5mM, pH8.0 in 75mM NaCl), DL-
234 Fluorocitric Acid (10mM, pH8.0 in 75mM NaCl) as Na⁺ salts, ejected as anions, with 2,2,2-Trifluoro-N-
235 [4-(2-methoxyphenoxy)phenyl]-N-(3-pyridinylmethyl)ethanesulfonamide hydrochloride (LY487379;
236 1mM, pH6.0, in 1% dimethyl sulfoxide [DMSO], 75mM NaCl ejected as cations. All compounds were
237 prevented from diffusing out of the pipette by using a retaining current (10-20nA) of opposite polarity
238 to that of the ejection current. Compounds were ejected within a current range ensured to produce a
239 sub-maximal effect on sensory inhibition (LY354740 6nA-50nA; LY487379 50nA-100nA) or neuronal
240 excitation (NMDA 35nA-85nA). Fluorocitrate was obtained from Sigma (St Louis, MO, USA), with all
241 other compounds obtained from Tocris (Bristol, UK). It is of importance to note that both the Group II
242 orthosteric agonist LY354740 (Monn *et al.*, 1997) and the mGlu2 positive allosteric modulator (PAM)
243 LY487379 (Schaffhauser *et al.*, 2003) used in this study possess a higher selectivity for their receptor
244 targets than the prototypical Group II orthosteric antagonist (2S)-2-Amino-2-[(1S,2S)-2-
245 carboxycycloprop-1-yl]-3-(xanth-9-yl)propanoic acid (LY341495) (Kingston *et al.*, 1998), which has

246 been demonstrated to have antagonistic properties at both the Group II and Group III mGlu
247 receptors in a similar iontophoretic *in vivo* study (Cirone & Salt, 2001).

248

249 2.44 STIMULATION PROTOCOLS

250 Neurons were identified as VB neurons on the basis of stereotaxic location (Paxinos & Watson, 1998)
251 and responses to vibrissa deflection. Vibrissa deflection was performed using fine air-jets directed
252 through 23 gauge needles mounted on micro-manipulators positioned and orientated close to the
253 vibrissa to ensure deflection of a single vibrissa was achieved. Air-jets were electronically gated with
254 solenoid valves that produced a rising air pulse at the vibrissa 8ms after switching. Response latencies
255 were calculated from the start of the gating pulse. Using such an approach it is possible to use air-jets
256 to evoke an excitatory response from stimulation of a single vibrissa, as described previously (Salt,
257 1989). Prior to the beginning of each of the experimental protocols described below, the 'principal'
258 vibrissa (i.e. the vibrissa at the centre of the receptive field) for each neuron was identified. All
259 neurons recorded from were quiescent.

260 2.441 PROTOCOL 1

261 *The effects of the selective glial inhibitor fluorocitrate on VB neuronal responses to train*
262 *stimulation of vibrissae and iontophoretic NMDA application*

263 Cycles of sensory and NMDA stimulation were established and repeated continuously whilst
264 recording from neurons. Cycles (60s long) contained two types of stimuli consisting of 500-
265 1000ms duration trains (5-10Hz) of air-jets directed at the principal vibrissa, repeated 4 times
266 with a 4s interstimulus interval, followed by a single iontophoretic NMDA application (10s),
267 which was timed to provide a 15s interval either side of the sensory stimulations. After several
268 control cycles displaying consistent VB neuronal responses had been recorded, fluorocitrate
269 was iontophoretically ejected for 5-12min as required until a consistent effect of fluorocitrate
270 was observed. An inter-stimulus interval of 4s is sufficient to ensure that any post-stimulus

271 effects from either stimulus type are no longer apparent upon subsequent stimulation (Salt,
272 1989; Turner & Salt, 2003).

273

274

275 2.442 PROTOCOL 2

276 *The effects of the selective glial inhibitor fluorocitrate on Group II mGlu receptor modulation*
277 *of sensory inhibition*

278 Cycles of sensory stimulation (10s long) were established and repeated continuously whilst
279 recording from neurons. Cycles contained one type of stimulus consisting of 500-1000ms
280 duration trains (5-10Hz) of air-jets directed at the principal vibrissa. After several control
281 cycles displaying consistent neuronal responses had been recorded, LY487379 and LY354740
282 were iontophoretically ejected for 2-15mins as required, under normal conditions and in the
283 presence of fluorocitrate. After cessation of compound ejection, sensory stimulation cycles
284 were continued until VB neuronal responses had returned to their respective control levels.

285

286 2.45 DATA COLLECTION AND STATISTICAL ANALYSIS

287 Throughout the study, extracellular single neuron action potentials were gated, timed and counted
288 using a window discriminator, a CED1401 interface and Spike2 software (Cambridge Electronic Design,
289 Cambridge, UK), which recorded the output from the iontophoresis unit and also triggered the
290 iontophoretic and sensory stimuli sequences. Data were analysed by plotting post-stimulus time
291 histograms (PSTHs) from these recordings by counting the spikes evoked by either NMDA ejection or
292 sensory stimulation. Data are expressed as a percentage of control responses prior to compound
293 application (\pm SEM). Comparisons were made using Wilcoxon matched-pairs test ($p < 0.05$).

294 3.0 RESULTS

295 The pharmacological compounds used in this study are clearly crucial to the interpretation of the
296 results. LY354740 is the best-studied selective Group II orthosteric agonist (Monn *et al.*, 1997; Schoepp
297 *et al.*, 2003), and has been used extensively to reveal Group II mGlu receptor function in both
298 behavioural (Schoepp *et al.*, 2003; Nordquist *et al.*, 2008) and *in vitro/vivo* physiological (Flor *et al.*,
299 2002; Moldrich *et al.*, 2003; Copeland *et al.*, 2012) assays in rodent and human CNS models. LY487379
300 is a highly selective mGlu2 PAM, which possesses no intrinsic agonist activity but does enhance
301 responses to submaximal glutamate without activity at other receptors or ion channels (Johnson *et*
302 *al.*, 2003). LY487379 has been used in a number of pharmacological assays, including behavioural and
303 *in vitro/vivo* electrophysiological studies in the rodent CNS (Schaffhauser *et al.*, 2003; Galici *et al.*,
304 2005, Poisik *et al.*, 2005; Harich *et al.*, 2007; Hermes & Renaud, 2010; Nikiforuk *et al.*, 2010; Copeland
305 *et al.*, 2012). The orthosteric antagonist LY341495 has a relatively high selectivity with a nanomolar
306 potency for Group II mGlu receptor, with submicromolar potencies at all other mGlu receptor
307 subtypes (Kingston *et al.*, 1998; Schoepp *et al.*, 1999). However, the parameters used for LY341495 in
308 this study have been demonstrated previously to produce selective antagonism for the Group II mGlu
309 receptors (Kingston *et al.*, 1998).

310

311 3.1 mGLU2 RECEPTORS MODULATE SYNAPTIC TRANSMISSION AT THE TRN-VB SYNAPSE

312 Group II mGlu receptor activation has been previously demonstrated to depress VB neuron inhibitory
313 postsynaptic potentials (IPSPs) evoked upon stimulation of the TRN (Turner & Salt, 2003), and an
314 mGlu2 component to this Group II effect was recently described in an *in vivo* study (Copeland *et al.*,
315 2012). Therefore, we first determined whether mGlu2 receptor activation is able to modulate
316 inhibitory synaptic transmission at the TRN-VB synapse. One component that would contribute to IPSP
317 depression is direct inhibition of GABAergic vesicle fusion with the presynaptic TRN membrane. By
318 recording miniature inhibitory postsynaptic currents (mIPSCs) it is possible to examine the frequency
319 of spontaneous presynaptic quantal release events and so detect changes in transmitter release in the

320 absence of evoked synaptic activity. In the absence of endogenous mGlu2 receptor activation, a
321 sub-maximal concentration (30nM) of the Group II agonist LY354740 was able to reduce mIPSC
322 frequency compared to baseline when applied alone ($10.0 \pm 1.6\%$ reduction compared to control, $n=6$
323 from 6 slices, **FIG. 2**). Application of the mGlu2 PAM LY487379 alone had no effect on mIPSC frequency
324 (data not shown). By nature of design, PAMs potentiate the action of orthosteric agonists, without
325 themselves possessing any intrinsic agonist activity (Johnson *et al.*, 2003). This lack of effect of the
326 PAM in this preparation is therefore unsurprising as there is likely no baseline activation of mGlu2
327 receptors under these conditions. However, when the mGlu2 PAM was co-applied with the sub-
328 maximal concentration of Group II agonist, a significant additional reduction in mIPSC frequency was
329 observed (30nM LY354740 & 30 μ M LY487379: $34.6 \pm 5.2\%$ reduction, $n=6$ from 6 slices, $p < 0.001$, **FIG.**
330 **2**), comparable to that seen upon maximal agonist effect (100nM LY354740: $39.1 \pm 4.7\%$ reduction
331 compared to control, $n=6$ from 6 slices, $p < 0.001$; **FIG. 2**). The Group II mGlu receptor effect on mIPSC
332 frequency was confirmed by its reversal upon Group II orthosteric antagonist LY341495 co-application
333 (100nM LY354740 & 100nM LY341495: $6.6 \pm 7.5\%$ reduction in mIPSC frequency compared to control,
334 $n=6$ from 6 slices, $p < 0.01$, **FIG. 2**). Taken together these data indicate that there is indeed an mGlu2
335 component to the Group II mGlu receptor effect on GABAergic transmission at the TRN-VB synapse.
336 Ultrastructural studies indicate that TRN terminals exclusively express the mGlu3 receptor subtype
337 (Tamaru *et al.*, 2001), while VB astrocytes express both mGlu2 and mGlu3 (Ralston, 1983; Ohara &
338 Lieberman, 1993; Liu *et al.*, 1998; Mineff & Valtschanoff, 1999). We therefore sought to confirm
339 functional expression of astrocytic mGlu2 receptors.

340

341 **3.2 MGLU2 RECEPTORS ACTIVATE ASTROCYTES IN THE VB**

342 Are mGlu2 receptors themselves able to directly activate astrocytes? To address this question, we
343 monitored intracellular calcium levels in both VB neurons and astrocytes in an acute *in vitro* thalamic
344 slice preparation. In the presence of TTX to block neuronal activity, a sub-maximal concentration of
345 the Group II orthosteric agonist induced increases in intracellular calcium levels compared to baseline
346 when applied alone (300nM, ratio amplitude 0.016 ± 0.002 , $n=56$ astrocytes from 5 slices, **FIG. 3a-c**).

347 Application of the mGlu2 PAM alone had no effect on intracellular calcium levels (data not shown).

348 Upon co-application of the mGlu2 PAM with the agonist there was a significant potentiation in

349 astrocytic intracellular calcium levels in the same astrocytes (300nM LY354740 plus 30 μ M LY487379,

350 ratio amplitude 0.035 ± 0.003 , $n=56$ astrocytes from 5 slices, $p<0.001$; **Fig. 3a-c**). This Group II mGlu

351 receptor effect could be reversed upon co-application of 1 μ M of the Group II antagonist LY341495

352 (1 μ M LY354740, 2.11 ± 0.45 $\Delta F\%$ change; 1 μ M LY354740 plus 1 μ M LY341495, $0.28\pm 0.17\Delta F\%$ change,

353 $n=10$ astrocytes from 5 slices, $p<0.01$; **Fig. 3d**). Co-application of the Group II agonist with 5 μ M 2-

354 Methyl-6-(phenylethynyl)pyridine (MPEP) and 100 μ M suramin had no effect (1 μ M LY354740 alone,

355 3.14 ± 0.30 $\Delta F\%$ change; 1 μ M LY354740 plus 5 μ M MPEP and 100 μ M suramin, 2.96 ± 0.30 $\Delta F\%$ change,

356 $n=106$ astrocytes from 4 slices; **Fig. 3d**), ruling out any mGlu5 or purine receptor involvement.

357 Furthermore, there was no change in the intracellular calcium levels in neurons in the same slices

358 when a maximal concentration of the Group II orthosteric agonist was applied alone (1 μ M, ratio

359 amplitude 0.004 ± 0.006 , $n=36$ neurons from 3 slices; **Fig. 3a-c**) nor when co-applied in the same slices

360 with the mGlu2 PAM (1 μ M LY354740 plus 30 μ M LY487379, ratio change 0.005 ± 0.003 , $n=36$ neurons

361 from 3 slices, $p>0.05$; **Fig. 3a-c**). G_q -protein coupled receptor-dependent calcium fluxes in astrocytes

362 are a result of the inositol-1,4,5-triphosphate receptor (IP3R) activation resulting in the release of

363 endoplasmic reticulum calcium ions into the cytosol (Sharp *et al.*, 1999; Holtzclaw *et al.*, 2002; Hertle

364 and Yeckel, 2007; Petravicz *et al.*, 2008). Astrocytes predominantly express the IP3R2 subtype

365 (Petravicz 2008). We therefore tested the effects of the mGlu2 agonist on acute slices from IP3R2 -/-

366 knockout mice. A maximal concentration (1 μ M) of the orthosteric agonist LY354740 was applied to

367 Fluo-4 loaded slices from wild-type (IP3R2+/+) and knock-out (IP3R2-/-) mice. A maximal

368 concentration of glutamate (100 μ M) that also activates other calcium signalling pathways such as

369 ionotropic receptors was subsequently applied to the same slice to provide an internal control. In

370 slices from wild-type animals, both LY354740 and glutamate elicited robust astrocyte calcium

371 elevations (LY354740: $5.12\pm 0.65\%$, Glutamate 7.41 ± 0.60 , $n=188$ astrocytes, 6 slices). However in slices

372 from knock-out mice, while glutamate elicited calcium elevations ($5.60\pm 0.35\%$), responses to

373 LY354730 were abrogated ($1.05\pm 0.18\%$, $n=100$ astrocytes from 5 slices **Fig. 3e**). The initial Ca^{2+} peak

374 induced by glutamate is abolished in the IP3R2 knock-out preparation, and can likely be attributed to

375 Group I mGluR activation, whose signal transduction pathway is mediated via Gq. The remaining
376 glutamate effect in the IP3R2 knock-out preparation can be attributed largely to activation of
377 ionotropic glutamate receptors (Höft et al., 2014), as application of ionotropic glutamate receptor
378 antagonists (NBQX and D-AP5) reduced the calcium associated fluorescence by 79% (data not shown);
379 whilst the initial Ca²⁺ peak, abolished, and this can likely be attributed to Group I mGluR activation.
380 Together, these data show that mGlu2 receptors elicit functional astrocyte responses via IP3R2
381 mediated calcium release; an effect traditionally associated with G_{q/11} coupled metabotropic
382 receptors, as opposed to the G_{i/o} coupled mGlu2 receptor. However, the same metabotropic receptor,
383 when expressed in different cell types/brain areas, is able to couple with alternate G-proteins: GABA_B
384 receptors have been reported to couple to both G_{i/o} and G_q (Gould *et al.*, 2014; Mariotti *et al.*, 2016)
385 and D1 receptors to G_s, G_{olf} and G_q proteins (Lee *et al.*, 2004). Furthermore, GABA_B receptor activation,
386 usually assumed to be coupled via G_{i/o}, induces calcium elevations in VB thalamus (Gould *et al.*, 2014).
387 As well as confirming an astrocytic locus for thalamic mGlu2 action, this represents a novel mechanism
388 of astrocytic activation.

389

390 **3.3 ASTROCYTES GATE NEURONAL RESPONSES TO SOMATOSENSORY STIMULATION**

391 Does this mechanism modulate thalamocortical responses to sensory stimulation in an *in vivo* system
392 (**FIG. 4A**)? To test this question, we first assessed whether astrocytes contribute to the generation of
393 VB neuron responses to physiological somatosensory stimulation. A recording electrode with
394 iontophoretic capabilities was advanced into the VB of rats, and vibrissae were deflected as required
395 to generate physiologically relevant activity. Observed waveforms were similar to those previously
396 published (Salt, 1989), and were not perturbed under experimental conditions. Fluorocitrate
397 selectively inhibits glia by interfering with the astrocytic tricarboxylic acid cycle (Fonnum *et al.*, 1997),
398 which is used to generate energy in the form of guanosine triphosphate (GTP). Upon local application
399 of fluorocitrate, a reduction in neuronal responses to repetitive 10Hz stimulation (1s duration) of the
400 principal vibrissae was observed. Specifically, the maintained component of the neuronal response
401 profile was significantly reduced (68±4% of control, n=16 from 9 rats, *p*<0.001), whereas the initial

402 component remained unaffected ($101\pm 3\%$ of control, $n=16$ from 9 rats, $p>0.05$) (**FIG. 4B,C**). The
403 maintained component of neuronal responses to vibrissa stimulation comprises an NMDA-mediated
404 contribution under normal physiological conditions (Salt, 1986). However, neuronal responses to
405 exogenous NMDA application were unaffected in the presence of fluorocitrate ($102\pm 4\%$ of control,
406 $n=11$ from 5 rats, $p>0.05$) (**FIG. 4B RIGHT PANELS; FIG. 4C**), thus indicating that inhibition of astrocyte
407 function does not impact directly on NMDA receptor responses or upon post-synaptic neuronal
408 excitability. Furthermore, as the initial component of neuronal responses to vibrissa stimulation was
409 reliably present upon each stimulus presentation (see raster plot in **FIG. 4B**) the impact of fluorocitrate
410 on neurotransmitter release can be considered minimal. The reduction of the maintained neuronal
411 response component to vibrissae stimulation observed in the presence of fluorocitrate could
412 therefore be attributable to the attenuation of an astrocytic mechanism of synaptic modulation
413 independent of a direct effect on the postsynaptic VB neuron.

414

415 **3.4 mGLU2 RECEPTORS MODULATE SYNAPTIC TRANSMISSION AT THE TRN-VB SYNAPSE VIA AN ASTROCYTE-** 416 **DEPENDENT MECHANISM**

417 Consistent with previous findings (Copeland *et al.*, 2012), local application of both the Group II
418 orthosteric agonist LY354740 and the mGlu2 PAM LY487379 were able to significantly increase
419 neuronal responses to 10Hz train stimulation of principal vibrissae under normal conditions
420 (LY354740: $156\pm 12\%$ of control, $n=6$ from 4 rats, $p<0.05$; LY487379: $144\pm 10\%$ of control, $n=6$ from 6
421 rats, $p<0.05$; **FIG. 5A**). However, in the same population of neurons in the presence of fluorocitrate,
422 the effect of the mGlu2 PAM was completely abolished ($91\pm 5\%$ of fluorocitrate control, $n=6$ from 4
423 rats, $p>0.05$; **FIG. 5B**) whereas the Group II mGlu receptor orthosteric agonist effect remained ($156\pm 9\%$
424 of fluorocitrate control, $n=6$ from 6 rats, $p<0.05$; **FIG. 5B**). Fluorocitrate inhibits formation of the energy
425 source GTP (Fonnum *et al.*, 1997), which is required for mGlu2 receptor signal transduction
426 (Niswender & Conn, 2010). From this selective attenuation of the mGlu2 PAM effect upon inhibition
427 of astrocyte function we can infer that mGlu2 receptor modulation of the TRN-VB synapse function is
428 astrocyte-dependent. Furthermore, we can attribute the remaining Group II mGlu receptor

429 orthosteric agonist effect to activation of neuronal mGlu3 receptors localised on presynaptic TRN
430 terminals (Tamaru *et al.*, 2001; Turner & Salt, 2003). Thus we have now shown that mGlu2 receptor-
431 mediated effects upon somatosensory transmission within the VB are astrocyte dependent under
432 physiological conditions.

433 4.0 DISCUSSION

434 By using selective pharmacological tools in complementary *in vitro* and *in vivo* preparations we have
435 been able to identify a novel mechanism of mGlu2 receptor-mediated astrocytic activation. In
436 summary, our *in vitro* experiments showed that selective potentiation of mGlu2 receptor activity
437 contributes to reducing inhibitory transmission at the TRN-VB synapse, and delineate the anatomical
438 localisation of these mGlu2 receptors to astrocytes, whose processes are known to co-localise with
439 TRN terminals on the soma and/or proximal dendrites of VB neurons (Ralston, 1983; Ohara &
440 Lieberman, 1993) (FIG. 6). Our *in vivo* experiments extend our *in vitro* findings, showing that selective
441 potentiation of mGlu2 receptor activity leads to an astrocyte-dependent increase in VB neuron
442 responsiveness to somatosensory stimulation in a physiological context. This mechanism likely occurs
443 upon physiological sensory stimulation as previously described, with the source of endogenous
444 glutamate being glutamate spillover from the sensory afferent terminals activating mGlu2 receptors
445 localised on the glial processes (Copeland *et al.*, 2012). Therefore, we provide the first evidence that
446 physiological activation of astrocytic mGlu2 receptors leads to concomitant modulation of thalamic
447 processing of sensory inputs. Furthermore, previously the mGlu3 and mGlu5 receptor subtypes have
448 been shown to be expressed in astrocytes (Niswender & Conn, 2010), with the mGlu5 subtype shown
449 to mediate sensory driven activation of thalamic astrocytes (Parri *et al.*, 2010). We have now shown
450 functional astrocytic mGlu2 receptors are also able to elicit an increase in astrocytic intracellular
451 calcium levels.

452

453 Whilst it has been previously demonstrated that astrocytes can act as a primary source of glutamate
454 (Parri *et al.*, 2001), we have now shown for the first time that astrocytes can themselves be activated
455 via mGlu2 receptors. The functional outcome of this mechanism facilitates disinhibition of the
456 postsynaptic VB neuron via action at the presynaptic TRN bouton, thus increasing the responsivity of
457 the VB neuron to sensory stimulation, as opposed to providing a direct postsynaptic excitatory
458 innervation (Parri *et al.*, 2001). We are able to delineate this by drawing together results from different
459 experimental paradigms. Firstly, neither the selective glial inhibitor fluorocitrate nor the Group II

460 orthosteric agonist or mGlu2 PAM perturbed VB neuronal responses to exogenous NMDA
461 (Copeland *et al.*, 2012), indicating that neither normal astrocytic function nor Group II/mGlu2 receptor
462 activation directly impinges upon the postsynaptic excitability of the VB neuron. The latter of these
463 results also provides evidence against the involvement of somatodendritically expressed mGlu2
464 receptors (Watanabe & Nakanishi, 2003), which corresponds with ultrastructural evidence indicating
465 a lack of Group II mGlu receptor expression by sensory thalamic neurons (Alexander & Godwin, 2006).
466 Furthermore, Group II mGlu receptor activation reduces IPSPs evoked in VB neurons upon stimulation
467 of the TRN without an effect on postsynaptic membrane properties in an *in vitro* thalamic slice
468 preparation (Turner & Salt, 2003), indicative of a presynaptic mechanism of action. Taken together,
469 these results indicate that astrocytic mGlu2 receptors act to modulate sensory-evoked inhibition in
470 the VB via a mechanism independent of a direct effect on the postsynaptic neuron, and is therefore
471 likely a presynaptic mechanism acting to reduce inhibitory synaptic transmission from the TRN to the
472 VB. Indeed, astrocytes have been shown to release adenosine, which can lead to the opening of
473 neuronal potassium channels (Winder *et al.*, 1996) and subsequent modulation of neuronal
474 excitability and action potential propagation. This mechanism of astrocyte-neuron signalling would
475 thus reduce calcium influx at the TRN terminal and subsequent vesicle fusion with the presynaptic
476 membrane. Such a non-neuronal dependent component of synaptic transmission could be occurring
477 upon activation of astrocytic mGlu2 receptors (**FIG. 6**).

478

479 We are also able to infer that there is an mGlu3 receptor component to the overall Group II mGlu
480 receptor activity on reducing inhibitory synaptic transmission at the TRN-VB synapse: when examining
481 the *in vivo* electrophysiological data, whilst the selective glial inhibitor fluorocitrate was able to
482 eliminate the mGlu2 PAM effect on sensory-evoked inhibition in the VB, there was a remaining Group
483 II orthosteric agonist effect, indicative of an mGlu3 receptor component likely mediated by neuronal
484 mechanisms. Indeed, there is anatomical evidence that mGlu3, but not mGlu2, receptors are located
485 on TRN terminals within the VB (Tamaru *et al.*, 2001), and that they are able to increase responses to
486 sensory stimulation via a reduction in inhibition arising from the TRN (Turner & Salt, 2003). The

487 function of these presynaptic mGlu3 receptors, which inhibit GABAergic transmission from the TRN
488 by increasing K⁺ conductance (Alexander and Godwin, 2006; Cox and Sherman, 1999), is opposite to
489 that of Group I mGlu receptors (mGlu1 & mGlu5), which depolarise TRN neurons by decreasing K⁺
490 conductance (Cox and Sherman, 1999) and activating a Ca²⁺-dependent non-selective cation
491 conductance (Neyer *et al.*, 2016). This duality in glutamatergic signalling would suggest a state-
492 dependent reciprocal role of glutamate within the VB-TRN complex, which may act in concert to
493 support complex behaviours. It is important to note that there is also evidence from ultrastructural
494 studies that indicate both Group II mGlu receptors may be localised on glial processes surrounding the
495 TRN-VB synapse (Ralston, 1983; Ohara & Lieberman, 1993; Liu *et al.*, 1998; Mineff & Valtschanoff,
496 1999). However, due to a lack of commercially available mGlu3 selective ligands, we are unable to
497 investigate whether there is an mGlu3 astrocytic component to the overall Group II mGlu receptor
498 effect on sensory-evoked inhibition in the VB.

499

500 5.0 CONCLUSIONS

501 In conclusion, our findings, at the cellular and network levels, provide causal support for the
502 hypothesis that mGlu2 receptor modulation of the TRN-VB synapse is astrocyte dependent. This is the
503 first evidence that mGlu2 receptors are able to activate astrocytes, and represents a tripartite
504 signalling pathway that modulates sensory processing in the thalamus. The TRN is responsible for
505 ensuring synchronous activity across almost all functional modalities (Pinault, 2004) through inhibitory
506 and disinhibitory circuits. Modulation of thalamic inhibitory processing via this novel astrocyte-
507 dependent mechanism therefore represents an integral component of thalamic function thought to
508 be of importance in the control of sensory discriminative processes (Copeland *et al.*, 2012). This
509 mechanism likely functions within thalamic circuitry to enable relevant information to be discerned
510 from background activity, and would thus also be important in the understanding of synaptic
511 processes underlying attention and cognition. This mechanism may therefore be an important
512 potential therapeutic target in conditions where perturbed inhibitory systems have been
513 hypothesised as contributory factors, such as in epilepsy and schizophrenia (Huguenard, 1999; Rub *et*
514 *al.*, 2003; Barbas & Zikopoulos, 2007; Pinault, 2011).

515

516

517

518

519

520

521

522

523

524 **ACKNOWLEDGEMENTS**

525

526 The authors would like to thank the Biotechnology and Biological Sciences Research Council (BBSRC)
527 (BB/H530570/1 to TES; BB/J017809/1 to HRP) and Merck and Co. for funding this project. We also
528 thank Prof A Araque (University of Minnesota) and Prof J Chen (UC San Diego) for the gift of IP3R2 -/
529 mice.

530 REFERENCES

- 531
532 Alexander GM & Godwin DW. (2006). Unique presynaptic and postsynaptic roles of Group II
533 metabotropic glutamate receptors in the modulation of thalamic network activity.
534 *Neuroscience* **141**, 501-513.
- 535
536 Barbas H & Zikopoulos B. (2007). The prefrontal cortex and flexible behavior. *Neuroscientist* **13**, 532-
537 545.
- 538
539 Cirone J & Salt TE. (2001). Group II and III metabotropic glutamate receptors contribute to different
540 aspects of visual response processing in the rat superior colliculus. *J Physiol* **534**, 169-178.
- 541
542 Cox CL & Sherman SM. (1999). Glutamate inhibits thalamic reticular neurons. *J Neurosci* **19**, 6694-
543 6699.
- 544
545 Copeland CS, Neale SA & Salt TE. (2012). Positive allosteric modulation reveals a specific role for mGlu2
546 receptors in sensory processing in the thalamus. *J Physiol* **590**, 937-951.
- 547
548 Crabtree JW. (1999). Intrathalamic sensory connections mediated by the thalamic reticular nucleus.
549 *Cell Mol Life Sci* **56**, 683-700.
- 550
551 D'Ascenzo M, Fellin T, Terunuma M, Revilla-Sanchez R, Meaney DF, Auberson YP, Moss SJ & Haydon
552 PG. (2007). mGluR5 stimulates gliotransmission in the nucleus accumbens. *Proc Natl Acad Sci*
553 *U S A* **104**, 1995-2000.
- 554
555 Fellin T, Pascual O, Gobbo S, Pozzan T, Haydon PG & Carmignoto G. (2004). Neuronal synchrony
556 mediated by astrocytic glutamate through activation of extrasynaptic NMDA receptors.
557 *Neuron* **43**, 729-743.
- 558
559 Fonnum F, Johnsen A & Hassel B. (1997). Use of fluorocitrate and fluoroacetate in the study of brain
560 metabolism. *Glia* **21**, 106-113.
- 561
562 Gould T, Chen L, Emri Z, Pirttimaki T, Errington AC, Crunelli V & Parri HR. (2014). GABA_B receptor-
563 mediated activation of astrocytes by gamma-hydroxybutyric acid. *Philos Trans R Soc Lond B*
Biol Sci **369**, 20130607.
- 564
565 Grosche J, Matyash V, Moller T, Verkhratsky A, Reichenbach A & Kettenmann H. (1999). Microdomains
566 for neuron-glia interaction: parallel fiber signaling to Bergmann glial cells. *Nat Neurosci* **2**, 139-
567 143.
- 568
569 Guthrie PB, Knappenberger J, Segal M, Bennett MV, Charles AC & Kater SB. (1999). ATP released from
570 astrocytes mediates glial calcium waves. *J Neurosci* **19**, 520-528.
- 571
572 Houser CR, Vaughn JE, Barber RP & Roberts E. (1980). GABA neurons are the major cell type of the
573 nucleus reticularis thalami. *Brain Res* **200**, 341-354.

- 574
575 Höft S, Griemsmann S, Seifert G & Steinhäuser C. (2014). Heterogeneity in expression of functional
576 ionotropic glutamate and GABA receptor in astrocytes across brain regions: insights from the
577 thalamus. *Philos Tran R Soc London B Biol Sci* **369**, 20130602.
- 578 Huguenard JR. (1999). Neuronal circuitry of thalamocortical epilepsy and mechanisms of antiabsence
579 drug action. *Adv Neurol* **79**, 991-999.
- 580
581 Johnson MP, Baez M, Jagdmann GE, Jr., Britton TC, Large TH, Callagaro DO, Tizzano JP, Monn JA &
582 Schoepp DD. (2003). Discovery of allosteric potentiators for the metabotropic glutamate 2
583 receptor: synthesis and subtype selectivity of N-(4-(2-methoxyphenoxy)phenyl)-N-(2,2,2-
584 trifluoroethylsulfonyl)pyrid-3-ylmethylamine. *J Med Chem* **46**, 3189-3192.
- 585
586 Jones EG. (1985). *The Thalamus*. Raven, New York.
- 587
588 Kafitz KW, Meier SD, Stephan J & Rose CR. (2008). Developmental profile and properties of
589 sulforhodamine 101--labeled glial cells in acute brain slices of rat hippocampus. *J Neurosci*
590 *Methods* **169**, 84-92.
- 591
592 Kakei S, Na J & Shinoda Y. (2001). Thalamic terminal morphology and distribution of single
593 corticothalamic axons originating from layers 5 and 6 of the cat motor cortex. *J Comp Neurol*
594 **437**, 170-185.
- 595
596 Kingston AE, Ornstein PL, Wright RA, Johnson BG, Mayne NG, Burnett JP, Belagaje R, Wu S & Schoepp
597 DD. (1998). LY341495 is a nanomolar potent and selective antagonist of group II metabotropic
598 glutamate receptors. *Neuropharmacology* **37**, 1-12.
- 599
600 Lee SP, So CH, Rashid AJ, Varghese G, Cheng R, Lança AJ, O'Dowd BF & George SR. (2004). Dopamine
601 D1 and D2 receptor co-activation generates a novel phospholipase C-mediated calcium signal.
602 *J Biol Chem* **279**, 35671-25678.
- 603
604 Liu XB, Munoz A & Jones EG. (1998). Changes in subcellular localization of metabotropic glutamate
605 receptor subtypes during postnatal development of mouse thalamus. *J Comp Neurol* **395**, 450-
606 465.
- 607 Mariotti L, Losi G, Sessolo M, Marcon I & Carmiognoto G. (2016). The inhibitory neurotransmitter
608 GABA evoked long-lasting Ca(2+) oscillations in cortical astrocytes. *Glia* **64**, 363-373.
- 609
610 Mineff E & Valtschanoff J. (1999). Metabotropic glutamate receptors 2 and 3 expressed by astrocytes
611 in rat ventrobasal thalamus. *Neurosci Lett* **270**, 95-98.
- 612
613 Monn JA, Valli MJ, Massey SM, Wright RA, Salhoff CR, Johnson BG, Howe T, Alt CA, Rhodes GA, Robey
614 RL, Griffey KR, Tizzano JP, Kallman MJ, Helton DR & Schoepp DD. (1997). Design, synthesis,
615 and pharmacological characterization of (+)-2-aminobicyclo[3.1.0]hexane-2,6-dicarboxylic
616 acid (LY354740): a potent, selective, and orally active group 2 metabotropic glutamate
617 receptor agonist possessing anticonvulsant and anxiolytic properties. *J Med Chem* **40**, 528-
618 537.

- 619 Neyer C, Herr D, Kohmann D, Budde T, Pape HC & Coulon P. (2016). mGluR-mediated calcium
620 signalling in the thalamic reticular nucleus. *Cell Calcium* B59, **312-323**.
- 621 Niswender CM & Conn PJ. (2010). Metabotropic glutamate receptors: physiology, pharmacology, and
622 disease. *Annu Rev Pharmacol Toxicol* **50**, 295-322.
- 623
- 624 Ohara PT & Lieberman AR. (1985). The thalamic reticular nucleus of the adult rat: experimental
625 anatomical studies. *J Neurocytol* **14**, 365-411.
- 626
- 627 Ohara PT & Lieberman AR. (1993). Some aspects of the synaptic circuitry underlying inhibition in the
628 ventrobasal thalamus. *J Neurocytol* **22**, 815-825.
- 629
- 630 Panatier A, Theodosis DT, Mothet JP, Touquet B, Pollegioni L, Poulain DA & Oliet SH. (2006). Glia-
631 derived D-serine controls NMDA receptor activity and synaptic memory. *Cell* **125**, 775-784.
- 632
- 633 Parri HR & Crunelli V. (2001). Pacemaker Calcium Oscillations in Thalamic Astrocytes in Situ.
634 *Neuroreport* **12**, 3897-3900.
- 635
- 636 Parri HR, Gould TM & Crunelli V. (2001). Spontaneous astrocytic Ca²⁺ oscillations in situ drive NMDAR-
637 mediated neuronal excitation. *Nat Neurosci* **4**, 803-812.
- 638
- 639 Parri HR, Gould TM & Crunelli V. (2010). Sensory and cortical activation of distinct glial cell subtypes
640 in the somatosensory thalamus of young rats. *Eur J Neurosci* **32**, 29-40.
- 641
- 642 Paxinos G & Watson C. (1998). *The Rat Brain in Stereotaxic Co-ordinates*. Academic Press, San Diego,
643 CA.
- 644
- 645 Pinault D. (2004). The thalamic reticular nucleus: structure, function and concept. *Brain Res Brain Res*
646 *Rev* **46**, 1-31.
- 647
- 648 Pinault D. (2011). Dysfunctional thalamus-related networks in schizophrenia. *Schizophr Bull* **37**, 238-
649 243.
- 650
- 651 Pinault D & Deschenes M. (1998). Anatomical evidence for a mechanism of lateral inhibition in the rat
652 thalamus. *Eur J Neurosci* **10**, 3462-3469.
- 653
- 654 Porter JT & McCarthy KD. (1996). Hippocampal astrocytes in situ respond to glutamate released from
655 synaptic terminals. *J Neurosci* **16**, 5073-5081.
- 656
- 657 Ralston HHI. (1983). *The synaptic organization of the ventrobasal thalamus in the rat, cat and monkey.*
658 *In Somatosensory Integration in the Thalamus*. Elsevier Science, Amsterdam.
- 659
- 660 Rouiller EM, Tanne J, Moret V, Kermadi I, Boussaoud D & Welker E. (1998). Dual morphology and
661 topography of the corticothalamic terminals originating from the primary, supplementary
662 motor, and dorsal premotor cortical areas in macaque monkeys. *J Comp Neurol* **396**, 169-185.
- 663

- 664 Rub U, Del Turco D, Del Tredici K, de Vos RA, Brunt ER, Reifenberger G, Seifried C, Schultz C,
665 Auburger G & Braak H. (2003). Thalamic involvement in a spinocerebellar ataxia type 2 (SCA2)
666 and a spinocerebellar ataxia type 3 (SCA3) patient, and its clinical relevance. *Brain* **126**, 2257-
667 2272.
- 668
669 Salt TE. (1986). Mediation of thalamic sensory input by both NMDA receptors and non-NMDA
670 receptors. *Nature* **322**, 263-265.
- 671
672 Salt TE. (1987). Excitatory amino acid receptors and synaptic transmission in the rat ventrobasal
673 thalamus. *J Physiol* **391**, 499-510.
- 674
675 Salt TE. (1989). Gamma-aminobutyric acid and afferent inhibition in the cat and rat ventrobasal
676 thalamus. *Neuroscience* **28**, 17-26.
- 677
678 Salt TE & Turner JP. (1998). Modulation of sensory inhibition in the ventrobasal thalamus via activation
679 of group II metabotropic glutamate receptors by 2R,4R-aminopyrrolidine-2,4-dicarboxylate.
680 *Exp Brain Res* **121**, 181-185.
- 681
682 Schaffhauser H, Rowe BA, Morales S, Chavez-Noriega LE, Yin R, Jachec C, Rao SP, Bain G, Pinkerton AB,
683 Vernier JM, Bristow LJ, Varney MA & Daggett LP. (2003). Pharmacological characterization and
684 identification of amino acids involved in the positive modulation of metabotropic glutamate
685 receptor subtype 2. *Mol Pharmacol* **64**, 798-810.
- 686
687 Schoepp, DD, Wright RA, Levine LR, Gaydos B & Potter WZ. (2003). LY354740, an mGlu2/3 receptor
agonist as a novel approach to treat anxiety/stress. *Stress* **6**, 189-197.
- 688
689 Serrano A, Haddjeri N, Lacaille JC & Robitaille R. (2006). GABAergic network activation of glial cells
690 underlies hippocampal heterosynaptic depression. *J Neurosci* **26**, 5370-5382.
- 691
692 Shosaku A, Kayama Y, Sumitomo I, Sugitani M & Iwama K. (1989). Analysis of recurrent inhibitory
693 circuit in rat thalamus: neurophysiology of the thalamic reticular nucleus. *Prog Neurobiol* **32**,
694 77-102.
- 695
696 Tamaru Y, Nomura S, Mizuno N & Shigemoto R. (2001). Distribution of metabotropic glutamate
697 receptor mGluR3 in the mouse CNS: differential location relative to pre- and postsynaptic
698 sites. *Neuroscience* **106**, 481-503.
- 699
700 Turner JP & Salt TE. (2003). Group II and III metabotropic glutamate receptors and the control of the
701 nucleus reticularis thalami input to rat thalamocortical neurones in vitro. *Neuroscience* **122**,
702 459-469.
- 703
704 Watanabe D & Nakanishi S. (2003). mGluR2 postsynaptically senses granule cell inputs at Golgi cell
705 synapses. *Neuron* **39**, 821-829.
- 706
707 Winder DG, Ritch PS, Gereau RWt & Conn PJ. (1996). Novel glial-neuronal signalling by coactivation of
708 metabotropic glutamate and beta-adrenergic receptors in rat hippocampus. *J Physiol* **494 (Pt**
709 **3)**, 743-755.

710 AUTHOR CONTRIBUTIONS

711 CS Copeland conceived and designed experiments, collected, analysed and interpreted data, drafted
712 the article, and approved the final version to be submitted.

713 TM Wall collected, analysed and interpreted data, revised the article critically for important
714 intellectual content, and approved the final version to be submitted.

715 Sims RE collected, analysed and interpreted data, revised the article critically for important intellectual
716 content, and approved the final version to be submitted.

717 SA Neale conceived and designed experiments, revised the article critically for important intellectual
718 content, and approved the final version to be submitted.

719 E Nisenbaum conceived and designed experiments, revised the article critically for important
720 intellectual content, and approved the final version to be submitted.

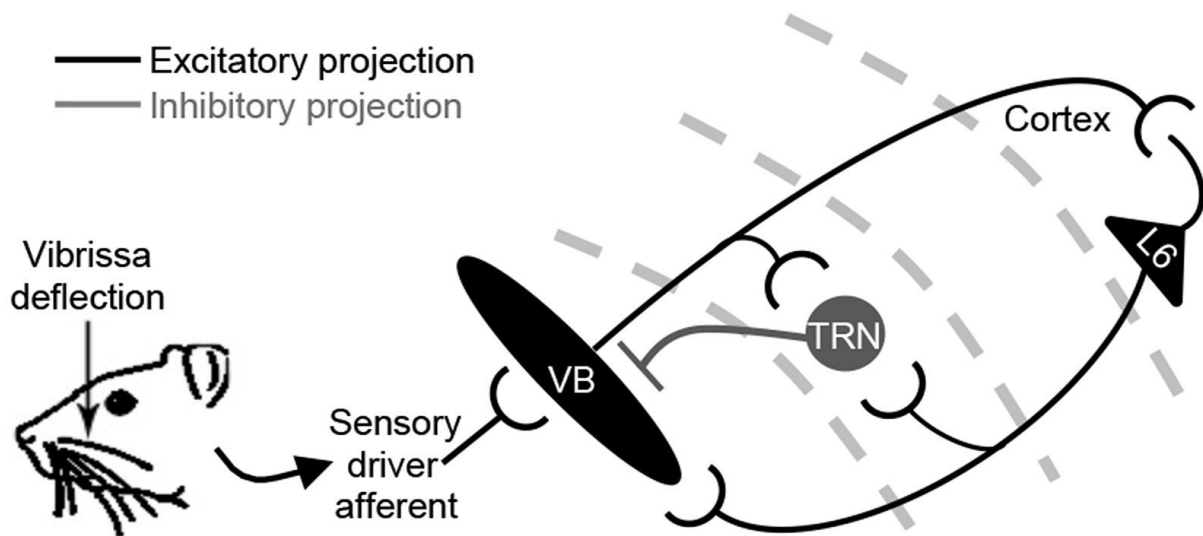
721 HR Parri conceived and designed experiments, collected, analysed and interpreted data, revised the
722 article critically for important intellectual content, and approved the final version to be submitted.

723 TE Salt conceived and designed experiments, revised the article critically for important intellectual
724 content, and approved the final version to be submitted.

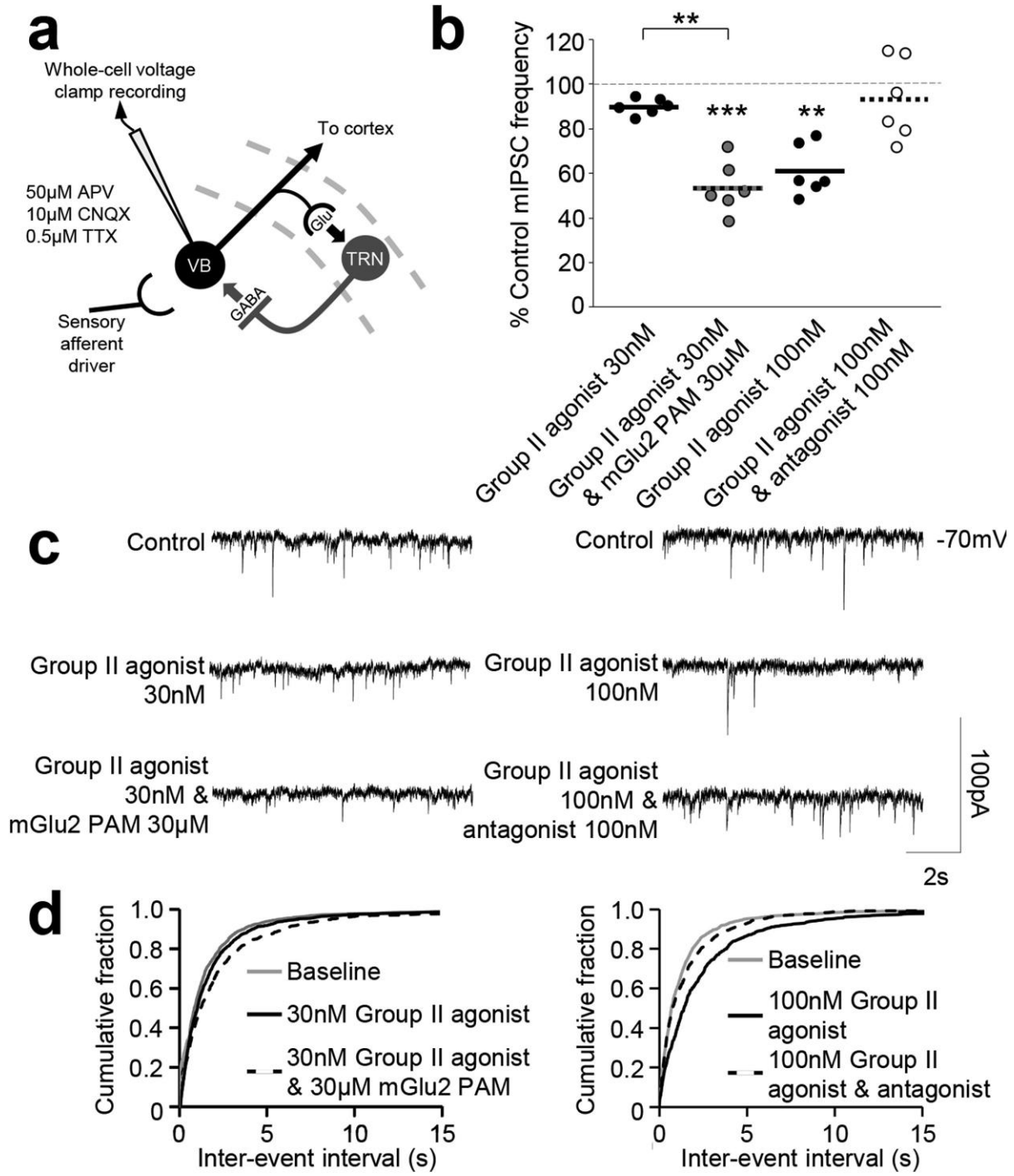
725 **FIGURE LEGENDS**

726 **FIGURE 1. Thalamic circuitry underlying responses to vibrissal deflection.** Branching collaterals from
 727 excitatory thalamocortical and corticothalamic axons (black), which originate from functionally linked
 728 topographical areas in the thalamus/cortex, innervate the TRN (Ohara & Lieberman, 1985; Shosaku *et al.*,
 729 *al.*, 1989; Rouiller *et al.*, 1998; Kakei *et al.*, 2001), and the TRN sends a reciprocal inhibitory projection
 730 (grey) back to the thalamic area from which it receives its thalamocortical innervation (Jones, 1985;
 731 Salt, 1989; Shosaku *et al.*, 1989; Pinault & Deschenes, 1998; Salt & Turner, 1998; Crabtree, 1999).

732

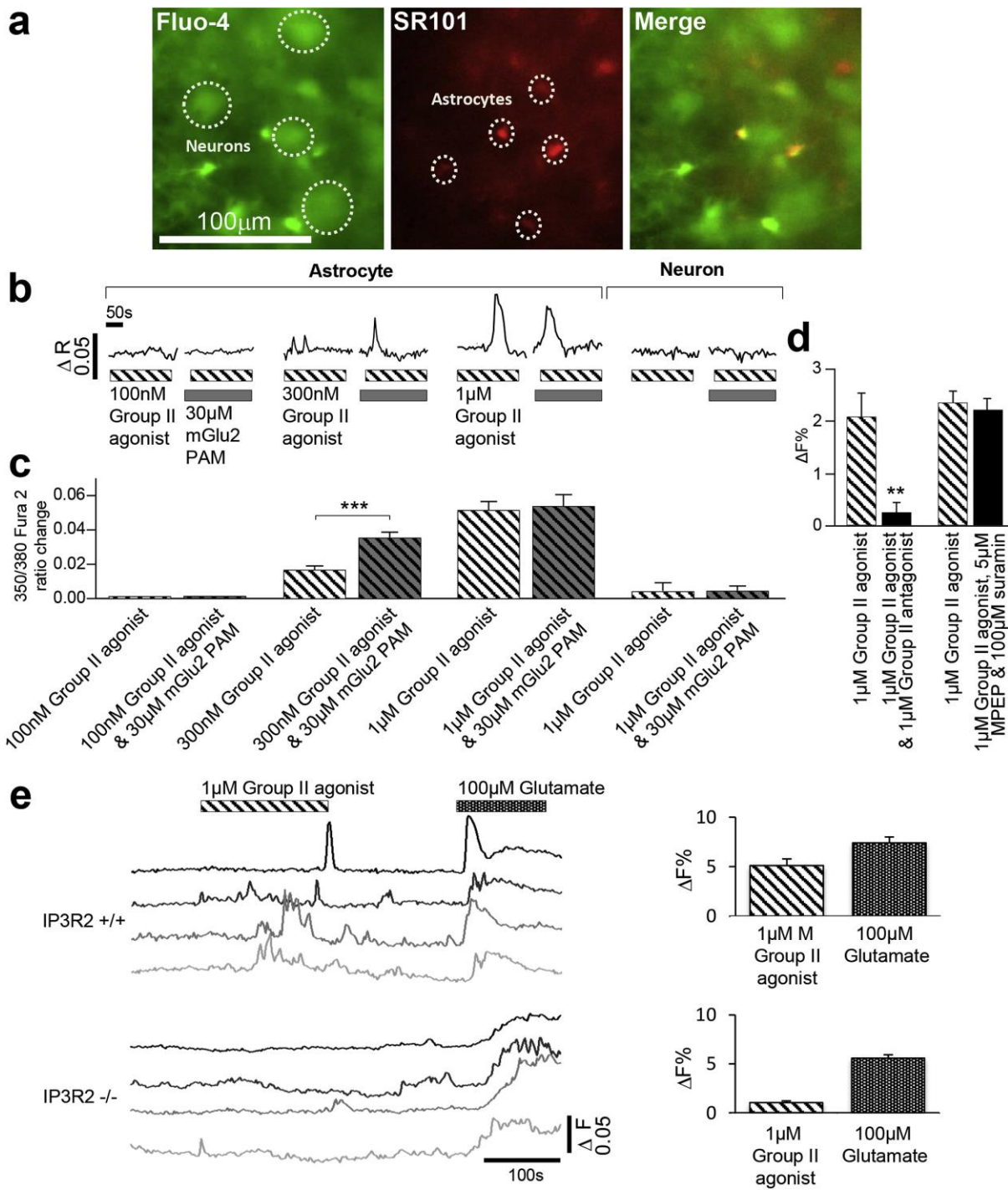


733 **FIGURE 2. The Group II mGlu receptor effect on spontaneous presynaptic quantal release events**
734 **includes an mGlu2 receptor-mediated component. a** Circuitry between the TRN and VB with
735 recording site indicated. **b** Effects of the Group II agonist LY354740 (30nM) alone or in conjunction
736 with the mGlu2 PAM LY487379 (30 μ M) on the total number of spontaneous mIPSC events (final 5
737 minute bin) in the VB. Specificity of the Group II agonist effect was confirmed upon its reversal using
738 the Group II antagonist LY341495 (100nM). **c** Traces from individual neurons illustrating the mean
739 responses of neurons to the same conditions as described in **b**. **d** Effects of the same compound
740 application combinations on the cumulative fraction of the calculated inter-event intervals of the
741 spontaneous mIPSCs in the VB. ** $p < 0.001$; *** $p < 0.0001$; Glu – glutamate.
742

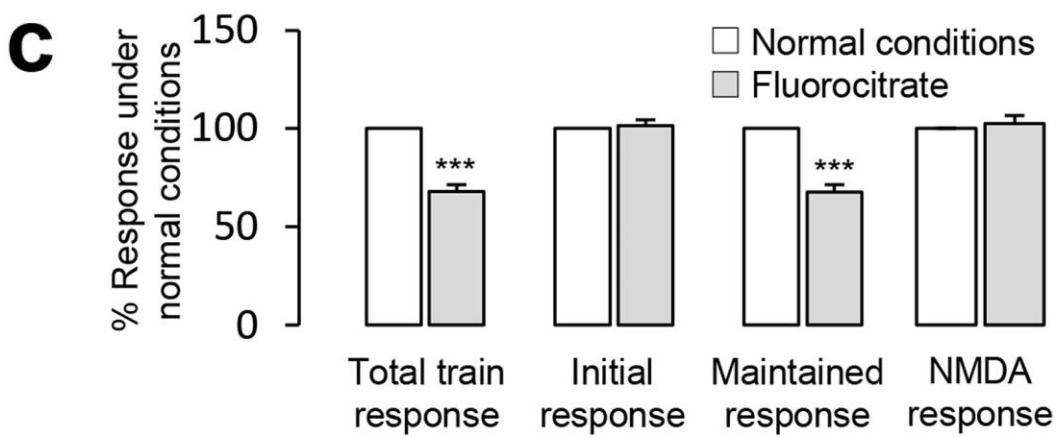
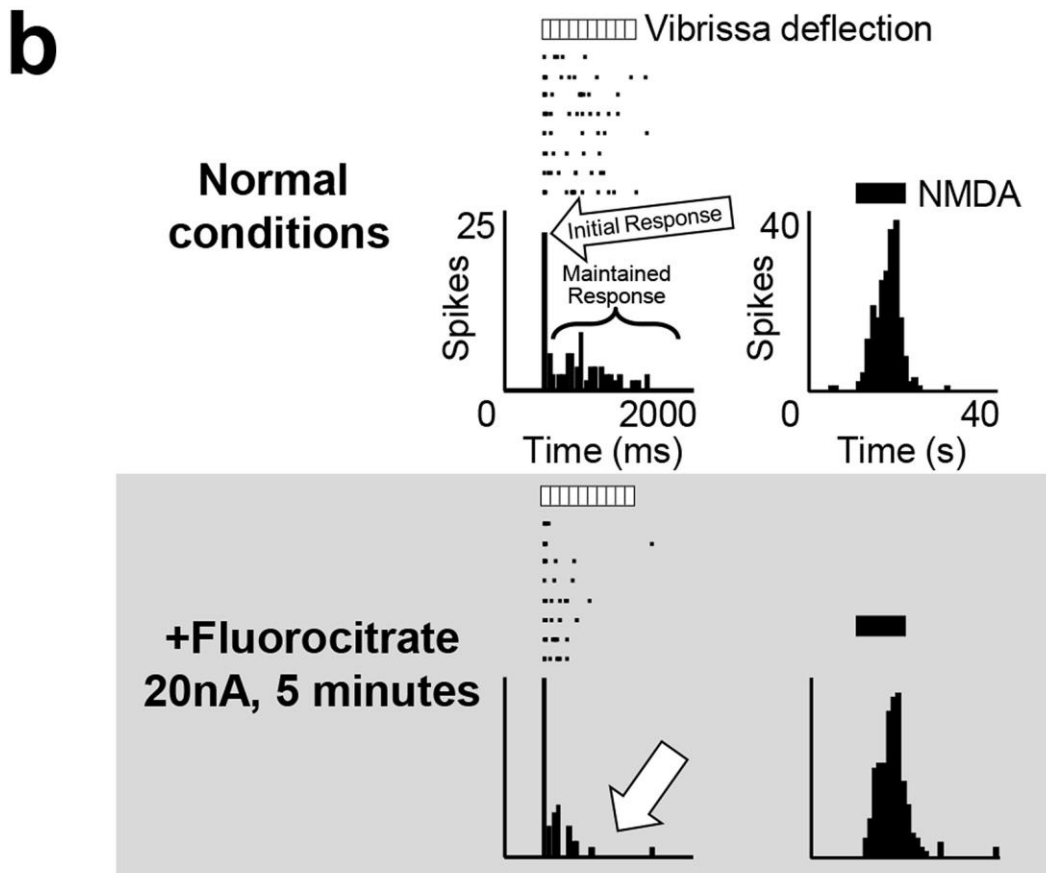
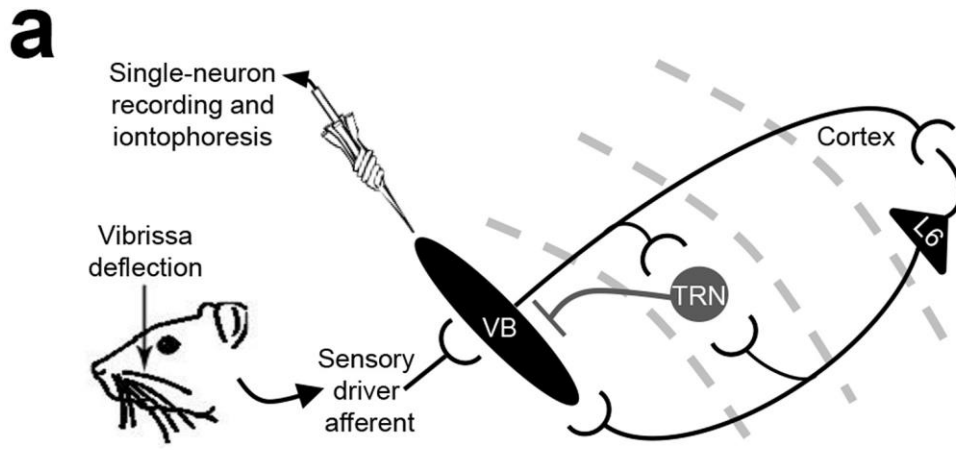


745 **FIGURE 3. mGlu2 receptor activation can elicit increases in astrocytic intracellular calcium levels. a**
746 Images from a slice loaded with Fluo-4-AM for calcium imaging, and SR101 for astrocyte
747 differentiation. Identified astrocytes and neurons are indicated. **b** Traces displaying transient
748 intracellular calcium elevations in an astrocyte in response to application of increasing concentrations
749 of the Group II agonist LY354740 either alone or in conjunction with the mGlu2 PAM LY487379. Two
750 traces on the right display ratio over time for example a neuron. **c** Bargraphs summarise results from
751 a number of experiments corresponding to the illustrative traces above in **b**. (Astrocytes: 100nM
752 LY354740 alone and co-applied with 30 μ M LY487379, 3 slices, n=21; 300nM LY354740 alone and co-
753 applied with 30 μ M LY487379, 5 slices, n=56; 1 μ M LY354740 alone and co-applied with 30 μ M
754 LY487379, 3 slices, n=49; Neuron: 1 μ M LY354740 alone and co-applied with 30 μ M LY487379, 3 slices,
755 n=36). Compound application is indicated by the striped (LY354740) and grey (LY4872379) bars. **d**
756 Bargraphs summarise results from a number of experiments demonstrating antagonism of the Group
757 II agonist effect. The two bars on the left display $\Delta F\%$ changes in calcium fluorescence upon application
758 of 1 μ M of the Group II agonist LY354740 alone and in conjunction with 1 μ M of the Group II antagonist
759 LY341495. The two bars on the right display $\Delta F\%$ changes in calcium fluorescence upon application of
760 1 μ M of the Group II agonist LY354740 alone and in conjunction with 5 μ M MPEP and 100 μ M suramin.
761 **e** Upper traces display fluorescence over time for four example astrocytes from a slice from a wild-
762 type (IP3R2+/+) mouse with responses to Group II agonist (1 μ M) and glutamate (100 μ M). Traces
763 below show responses from astrocytes in a slice from an IP3R2(-/-) knock-out mouse. Bargraphs to
764 the right summarise a number of experiments. Bars in **c** and **d** represent the mean % response (\pm SEM)
765 of the fluorescence, ** $p < 0.01$, *** $p < 0.001$.

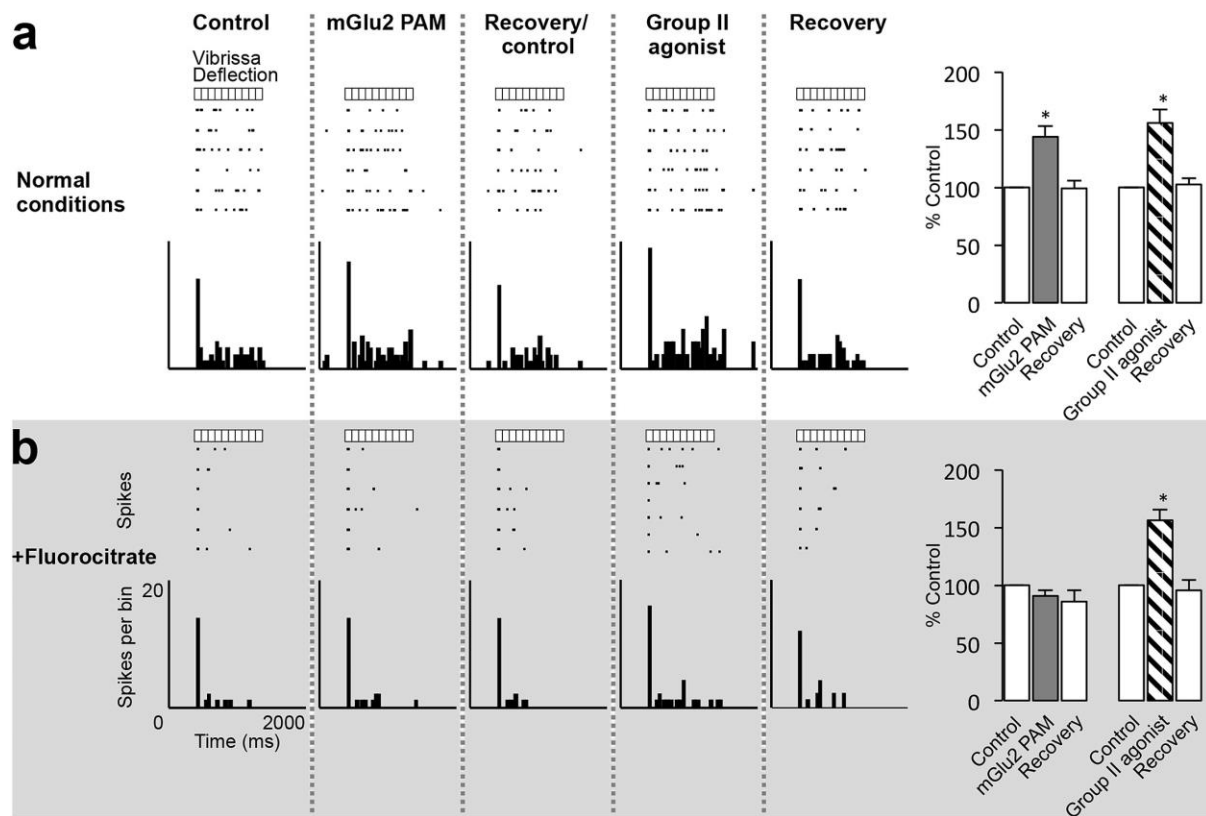
766



768 **FIGURE 4. Astrocyte inactivation attenuates the maintained component of VB neuron responses**
769 **without affecting responses to NMDA. a** Circuitry between the TRN and VB with recording site
770 indicated. **b** Raster displays and peristimulus time histograms (PSTHs) of responses of a VB neuron
771 (CVB142c) to either train stimulation of a single vibrissa (50ms bins, 8 trials) or iontophoretic
772 application of NMDA (15nA; 1s bins, 2 trials) under normal conditions and in the presence of
773 fluorocitrate (20nA; 5 minutes). **c** Bars represent the mean % response (\pm SEM) under normal
774 conditions (100%) and in the presence of fluorocitrate to train stimulation (total, initial and
775 maintained) of single vibrissae (n=16) and NMDA (n=11). *** $p < 0.001$.
776

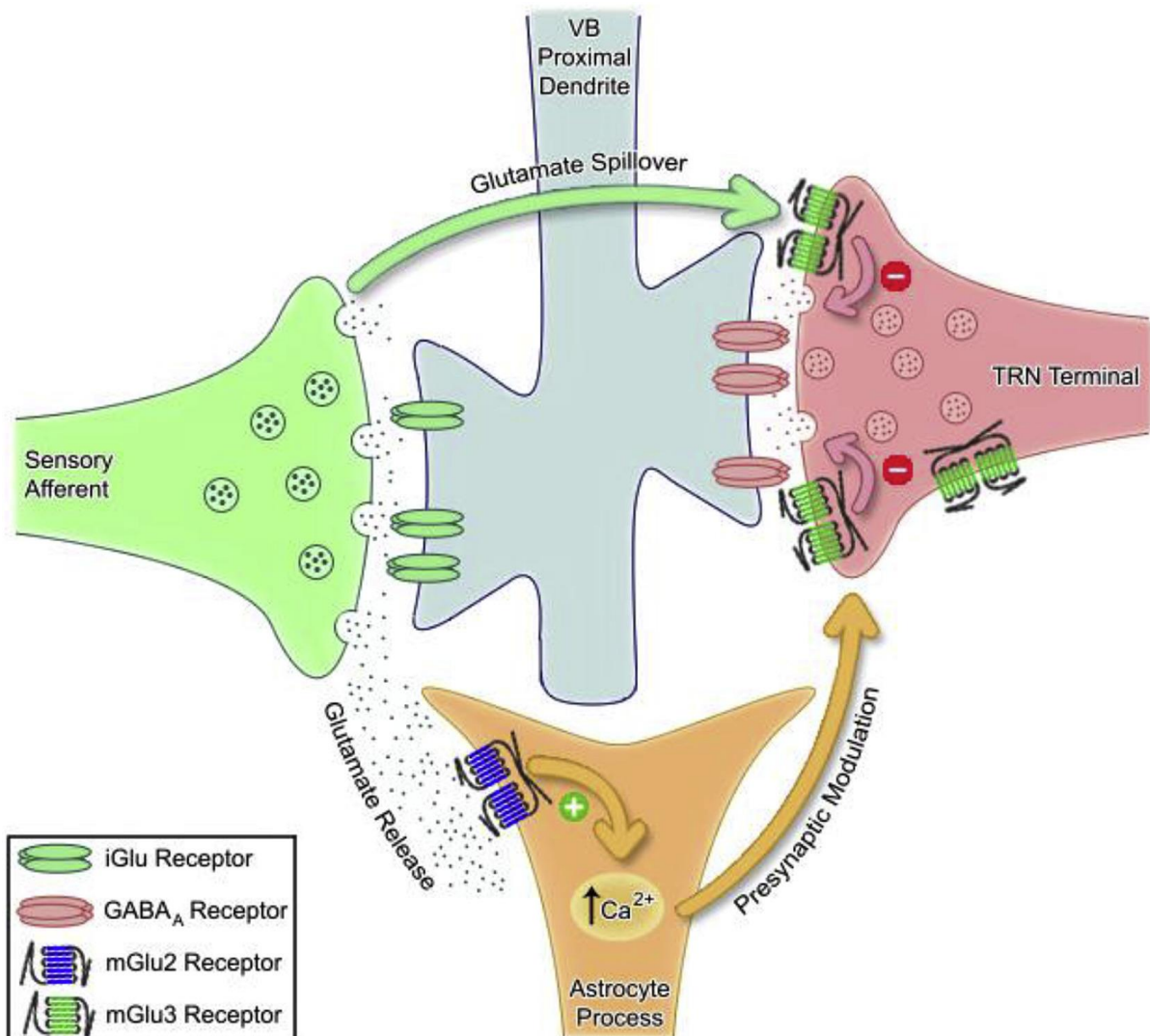


778 **FIGURE 5. Astrocyte inactivation attenuates the mGlu2 component of the Group II effect on**
 779 **sensory inhibition in the VB. a** Raster displays and PSTHs of responses of a VB neuron (CVB138a) to
 780 train stimulation (50ms bins, 6 trials) of a single vibrissa under normal conditions and in the presence
 781 of fluorocitrate (20nA; 10 minutes) during a control period, upon iontophoretic application of either
 782 LY487379 (50nA, 2 minutes) or LY354740 (50nA, 2 minutes), and during recovery. Abscissa indicated
 783 on the bottom left raster and PSTH plot applies to all plots. **b** Bars represent the mean % of control
 784 (\pm SEM) of responses to train stimulation of single vibrissae (n=6) to application of either LY487379 or
 785 LY354740 under normal conditions and in the presence of fluorocitrate. * $p < 0.05$.
 786



787

788 **FIGURE 6. Summary diagram of Group II mGlu receptor localizations in the VB, and their effects**
 789 **upon synaptic transmission.** Using selective pharmacological compounds, we have been able to show
 790 that mGlu2 receptors are likely located on astrocytic processes surrounding the TRN-VB synapse,
 791 whilst mGlu3 receptors are likely located on the TRN terminals themselves in the VB. Activation of
 792 astrocytic mGlu2 receptors likely facilitates elevations in intracellular calcium levels (indicated by a
 793 green plus), which may lead to presynaptic modulation of the TRN-VB synapse, whilst neuronal mGlu3
 794 receptor activation is thought to decrease GABAergic transmission (indicated by the red minus signs).
 795 Both of the Group II mGlu receptor subtypes are likely activated via glutamate spillover from the
 796 synapse formed between the sensory afferent and the VB proximal dendrite upon physiological
 797 sensory stimulation (Copeland et al., 2012).



798